

CHAPTER 193

A Design Short-Crested Wave Force Model for Vertical Deep-Water Breakwaters

S.-Y. Tzang¹ and S.-R. Liaw²

Abstract

Fenton's short-crested wave force approximations were modified for designing a vertical breakwater in deep water regions. The theoretical water surface profiles and depth-distributions of hydrodynamic pressure in front of a vertical breakwater were first evaluated with field wave conditions of height $H_b=10\text{m}$ and period $T=9.6\text{s}$ at depths d from 20m to 40m. The calculations immediately illustrated characteristics of residual pressures at wave crest and exponentially decreasing profiles under design water level. As d increased, wave crest height decreased as well and the crest pressure deviations became negligible while overestimated pressure force by assuming linear under-water pressure distributions became more significant. Through appropriate modifications, a design wave force model were proposed and compared with Goda's design formulae for standing waves. Results clearly displayed that 45° incident short-crested waves could induce greater total wave forces on a vertical breakwater than those by Goda's formulae at the same depth. Differences became greater at $d=40\text{m}$ by about 12% ~ 17% for $T=10\text{s}$ and 17% ~ 29% for $T=18\text{s}$ based on Fenton's 2nd and 3rd-order approximations.

Introduction

Currently in many countries, up-surgling economic developments have made breakwaters, which were used to be constructed at water depths around 20m, now tend to be installed at water depths of more than 40m. For example in Japan, several port engineering require rather deep water breakwaters such as those in port Kamaish (deepest depth of 63m) etc.(Tanimoto & Takahashi, 1994). Similar challenges are also about to be encountered in Taiwan for its deep-water port projects in the near future. Thus, studies on the complex wave characteristics before a breakwater and

¹ Associate Professor, Dept. of Harbor and River Eng. National Taiwan Ocean University, Keelung, Taiwan 202, R.O.C.

² Chief Engineer, Harbor & Coastal Eng. Dept., China Eng. Consultants, Inc. 20th Fl., 185 Hsin-Hai Rd. Sec. 2, Taipei, Taiwan, R.O.C

related engineering techniques have become an urgent task.

In marine environments, waves generally attack breakwaters obliquely rather than normally resulting in a short-crested wave system (Jeffrey, 1924; Chappellear, 1961). It has been a common engineering assumption adopted for design purposes that normal incident wave forces are greatest than short-crested wave forces, e.g. Goda's formulae (1972, 1985). In fact, this is not always true as pointed out previously that short-crested waves could induce greater wave forces on vertical walls than standing waves (Silvester, 1974; Roberts and Schwartz, 1983). These findings simply suggested that in certain conditions Goda's formulae for standing waves might under-estimate the resulting total wave forces and the designed breakwaters are more susceptible to catastrophic damages during storm attacks.

Goda's Design Wave Force Formulae

As schematically represented by Figure 1 for a composite breakwater, Goda defined wave crest height η_c and wave pressures P_i at specified positions as follows :

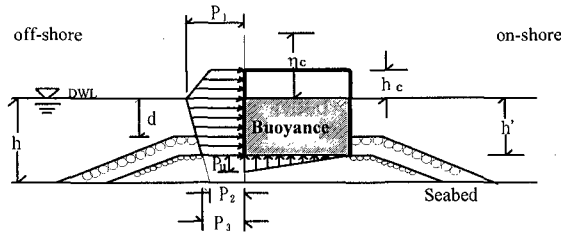


Figure 1. Definition Sketch of Goda's Design Standing Wave Pressures

Wave crest elevations

$$\eta_c = 0.75(1 + \cos \beta) \lambda H_{\max} \quad (1)$$

η_c : upper limit of wave pressure above design water level (DWL)

β : angle between incident wave and the normal of breakwaters

λ : pressure dissipation ratio (=1.0 for current paper)

Wave-induced pressures

$$P_1 = \frac{1}{2}(1 + \cos \beta)(\alpha_1 + \alpha_2 \cos^2 \beta) \lambda W_0 H_{\max} \quad ; \quad P_2 = \frac{P_1}{\cosh(2\pi h / L)}$$

$$P_3 = \alpha_3 P_1 \quad ; \quad P_u = \frac{1}{2}(1 + \cos \beta) \lambda \alpha_1 \alpha_3 w_0 H_{\max}$$

$$\alpha_1 = 0.6 + \frac{1}{2} \left[\frac{4\pi h / L}{\sinh(4\pi h / L)} \right]^2 \quad ; \quad \alpha_2 = \min \left\{ \frac{h_b - d}{3h_b} \left(\frac{H_{\max}}{d} \right)^2, \frac{2d}{H_{\max}} \right\} \quad (2)$$

$$\alpha_3 = 1 - \frac{h'}{h} \left[1 - \frac{1}{\cosh(2\pi h / L)} \right]$$

P_1, P_2, P_3, P_u : max. pressures at DWL, sea bed, caisson bottom and up lift pressure;

h, h', d : water depths from DWL to sea bed, caisson bottom, and rubble mound;

η_c, h_c : elevation of wave crest and caisson top above DWL;

$\alpha_1, \alpha_2, \alpha_3$: coefficients for pressure calculation.

For a vertical breakwater, it is shown that $h=d$ and $P_2=P_3$ while Eq.(1) and Eq.(2) confirm that Goda assumed maximum wave force by standing waves and those by obliquely incident waves decreased by a factor of $\cos\beta$.

Fenton's short-crested wave force theory

Based on Hsu et al's (1979) approximations of short-crested waves, Fenton (1985) further studied the surface wave profile, wave pressure and resulting total forces on a vertical wall. The short-crested wave system can be defined in Figure 2.

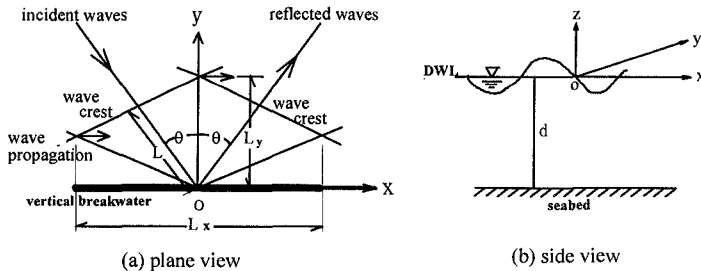


Figure 2. Definitions of A Short-Crested Wave System

As expressed in Figure 2, an obliquely incident wave and its reflected wave from a vertical wall can generate a short-crested wave system. Thus, short-crested waves are essentially three dimensional rather than the two dimensional standing waves, which approach a breakwater normally. According to Fenton in the case of total reflection, short-crested wave height H_{sc} is exactly equal to twice of the incident wave height H_D . Represented by Cartesian coordinates, the governing equation for the velocity potential ϕ simply satisfies the Laplace equation :

$$\nabla^2 \phi = \phi_{xx} + \phi_{yy} + \phi_{zz} = 0 \quad (3)$$

Solving with dynamic and kinematic boundary conditions on surface, at sea bed and on breakwater, Fenton derived a 3rd-order approximations with a variable $\delta = \frac{1}{2} k H_{sc}$ (H_{sc} : short-crested wave height) as expressed, respectively below :

Surface water profile :

$$k \eta(x, y, z, t) = \sum_{i=1}^3 \frac{\delta^i}{(i-1)!} \sum_{j=0}^i \cos j(mkx - \omega t) \sum_{l=0}^i B_{jil} \cos lnky + O(\delta^4) \quad (4)$$

Hydrodynamic pressure :

$$\frac{kp(x, y, z, t)}{\rho g} = -kz + \sum_{i=1}^3 \frac{\delta^i}{(i-1)!} \sum_{j=0}^i \cos j(mkx - \omega t) \sum_{l=0}^i C_{jil}(z) \cos lnky + O(\delta^4) \quad (5)$$

Total wave pressure force :

$$\begin{aligned} \frac{P^*}{\rho g d^2} &= \delta F_{11} \cos(mkx - \omega t) + \delta^2 [F_{20} + F_{22} \cos 2(mkx - \omega t)] \\ &+ \frac{1}{2} \delta^3 [F_{31} \cos(mkx - \omega t) + F_{33} \cos 3(mkx - \omega t)] + O(\delta^4) \end{aligned} \quad (6)$$

The dimensionless coefficients B_{ij} , C_{ij} , F_{ij} and the listed variables are all defined in Fenton (1985). To examine the short-crested wave characteristics before a vertical breakwater, both Fenton's 2nd and 3rd-order approximations shall be evaluated with field wave conditions and then modified for design applications. The results will also be compared with Goda's formulae to manifest the under-estimation of wave forces by standing wave theory in deeper water regions.

Wave Characteristics before A Deep-Water Vertical Breakwater

Both wave crest elevations and wave pressure at specified depths were first studied with a set of in-situ design wave conditions at installation depths of 20, 25, 30, 35, and 40m, respectively. The incident design wave height H_D is 10 meters, wave period T is 9.6 seconds and steady current along the breakwater is neglected in this paper. The seabed slope is assumed to be 1/50 for applying Goda's formulae and only incident angles $\theta=0.01^\circ$ and 45° were considered. Results calculated with water density $\rho=1.03 \text{ g/cm}^3$ and gravity acceleration $g=9.806 \text{ cm/s}^2$ are summarized in Table 1, where the shadowed areas denote results for $\theta=45^\circ$ by both approximations.

Water surface profiles

For water surface profiles, it is seen in Table 1 that short-crested wave crest heights η_c are decreasing with water depth and higher for normal incidence at each depth. The values at wave crest are exactly the same for both approximations but the phase variations of surface profiles are slightly different as illustrated in Figure 3. From both Table 1 and Figure 3, it is noted that short-crested η_c of both normal and oblique incidence are always smaller than those by Goda's formulae except for the case at $d=20\text{m}$. In fact, Goda's formulae gave a constant value of 15m regardless of the water depth and are even higher than short-crested waves by 1m to 2.9m at $d=40\text{m}$ for $\theta=0.01^\circ$ and 45° , respectively by different approximations.

Wave pressure depth distributions

Contrary to η_c , Table 1 shows that at each depth waves with the same height and period imposed greater maximum pressures for $\theta=45^\circ$ than those for normal incidence. This is clearly demonstrated by the phase variations of the wave pressure at half depth and seabed by both approximations as shown in Figure 4 and Figure 5, respectively. It is seen in both figures that maximum wave pressures of $\theta=45^\circ$ are greater than those of $\theta=0.01^\circ$ and maximum standing wave pressures occurred at phases deviated from phase of zero (wave crests) due to double hump structure. For waves of $\theta=45^\circ$, pressures at DWL and at seabed derived by 2nd-order approximation are all greater than those by 3rd-order approximation but the differences became quite small as water depth increased. By 2nd-order approximations, the residual errors of water pressure at wave crest tend to diminish with increasing depths except for the cases of $\theta=0.01^\circ$. This suggests that in deeper waters Fenton's approximations are more applicable due to negligibly small residual crest pressures and thus, resulting total wave pressure force on a vertical breakwater can be reasonably derived.

Table 1 Wave Characteristics by Fenton's and Goda's Approximations at Various Water Depths

$H_p=10\text{m}$, $T=9.6\text{sec}$, Slope= $1/50$ (for Goda's)

d=20m	θ	k	η_c	P_{crest}	P_1	$P_{1\text{max}}$	P_2	$P_{2\text{max}}$	d/L	H_{sc}/L	δ
3rd	0.01	0.058	15.61	52.75	40.40	52.28	8.44	46.69	0.185	0.184	0.578
	45	0.05	14.51	-75.35	68.48	*	50.04	*	0.159	0.160	0.503
2nd	0.01	0.058	15.61	192.30	109.20	*	48.30	*	0.185	0.184	0.578
	45	0.05	14.51	85.39	108.00	*	65.69	*	0.159	0.160	0.503
Goda's	0	0.055	15.0		72.93		43.71		$\alpha_1=0.72, \alpha_2=0.002$		
d=25m											
3rd	0.01	0.056	14.80	3.74	47.12	56.11	10.96	37.53	0.223	0.178	0.559
	45	0.048	13.35	-46.84	72.28	*	46.41	*	0.191	0.153	0.481
2nd	0.01	0.056	14.79	118.45	99.77	*	35.61	35.95	0.223	0.178	0.559
	45	0.048	13.35	34.13	94.50	*	52.85	*	0.191	0.153	0.481
Goda's	0	0.051	15		68.80		35.67		$\alpha_1=0.68, \alpha_2=0.0012$		
d=30m											
3rd	0.01	0.054	14.36	-7.56	51.18	57.86	9.64	30.64	0.258	0.172	0.540
	45	0.046	12.74	-29.71	74.41	*	41.08	*	0.220	0.146	0.459
2nd	0.01	0.054	14.36	86.54	95.10	*	26.45	28.58	0.258	0.172	0.540
	45	0.046	12.74	13.64	87.49	*	44.05	*	0.220	0.146	0.459
Goda's	0	0.049	15		65.72		28.7		$\alpha_1=0.65, \alpha_2=0.0007$		
d=35m											
3rd	0.01	0.052	14.12	-11.00	53.55	58.74	6.89	25.25	0.290	0.166	0.522
	45	0.045	12.37	-20.03	75.61	*	35.60	*	0.251	0.144	0.452
2nd	0.01	0.052	14.12	70.48	92.47	*	19.00	23.35	0.290	0.166	0.522
	45	0.045	12.37	3.56	83.34	*	37.06	*	0.251	0.144	0.452
Goda's	0	0.047	15		63.67		23.70		$\alpha_1=0.63, \alpha_2=0.0004$		
d=40m											
3rd	0.01	0.051	13.96	-12.15	55.07	59.26	3.88	21.41	0.325	0.160	0.503
	45	0.044	12.13	-14.28	76.30	*	30.44	*	0.280	0.140	0.440
2nd	0.01	0.051	13.96	61.48	90.93	*	12.91	19.63	0.325	0.160	0.503
	45	0.044	12.13	-2.07	80.70	*	31.20	*	0.280	0.140	0.440
Goda's	0	0.046	15		62.45		17.74		$\alpha_1=0.618, \alpha_2=0.0003$		

where

θ : incidence angle; k : wave number; η_c : wave crest elevation (unit: m); *: same as left

P_{crest} : wave pressure at η_c ; P_1, P_2 : wave pressure (phase $t/T=0$) at DWL & seabed

$P_{1\text{max}}, P_{2\text{max}}$: maximum wave pressure at DWL & seabed (unit: kN/m^2)

d/L : relative water depth; H_{sc}/L : short-crested wave steepness; δ : expansion parameter

Figure 6 and Figure 7 display both onshore and offshore pressures at different depths by both approximations, respectively. From the figures and Table 1, it is found that the residual errors at wave crest P_{crest} for 45° incident short-crested waves altogether decreased towards a theoretical zero to satisfy the Bernoulli assumptions at free surface boundary. The values decrease from 85 to -2 kN/m^2 by 2nd-order approximations and from -75 to -14 kN/m^2 by 3rd-order approximations at depths of 20m to 40m. For results by 2nd-order approximations, the deviations at wave crest seem more significant for normal incident waves than obliquely incident waves and pressure changes at DWL with depths were more notified than those by 3rd-order approximations. Being supported by negligible discrepancies between the two approximations at deep depths, it seems reasonable to apply either of the two approximations to estimate wave forces on a deep-water vertical breakwater.

Resultant wave forces estimations

Compared with the results by Goda's formulae, Table 1 shows that short-crested wave pressures of 45° incidence at DWL and seabed by both approximations were similarly greater than those by Goda's except at depth of 20m. The differences were gradually enlarged with increasing water depth at both locations, implying that Goda's formulae tend to under-estimate the resulting total pressure forces for obliquely incident waves on a deep water vertical breakwater. This is demonstrated with the calculated wave forces summarized in Table 2, in which numerical values were derived by summations of the approximated pressures directly from Eq.(6) at discretized depths. The reasons for utilizing discrete summations were mainly due to the avoidance of the residual effects of the surface errors on the resulting integration of Eq.(6) and the merits of estimations of wave forces between any two depths. Taking Figures 6 and 7 for illustrations, the pressure distributions above DWL were seen to be similarly linear for most depths but the surface residual errors would certainly cause calculated wave forces to be less reliable. If we correct this error by constraining the values of P_{crest} to be theoretically zero thus, wave forces can simply be calculated with known values of η_c and maximum pressure at DWL P_{1max} . However, this correction had resulted in an error equal to the triangle area with coordinates of $(P_{1max}, 0, P_{crest})$ and its magnitude is simply equal to $1/2 \times P_{crest} \times \eta_c$. Shown in Table 2, we notify the decreasing trends of the errors with increasing water depths since P_{crest} became much smaller as displayed in Figure 6 and 7. As a result, we found from Table 2 that errors are decreasing in deeper water by both approximations for 45° incident waves. However, the results for normal incidence have not shown similar tendency, rather are still significant at $d=30\text{m}$ and 40m , implying more attentions should be taken when applications.

On the other hand, the pressure force below DWL is simply the summation of the pressure force per unit depth. Usually for engineering applications as schematically shown in Figure 1 by Goda, the total on and off-shore pressure forces are derived by the magnitude of the area with linear distribution between P_1 and P_2 . The calculations are simple but may result in a significant error in resulting wave forces, especially for a deep water breakwater. As summarized in Table 2, the differences

between linear assumptions and the derived theoretical curves were exactly the shadowed areas shown in Figure 6 and 7. In this paper, the theoretical under-water total forces were approximated by summations of 20 trapezoidal pressure forces and more divisions can only slightly change the results. Obviously, linear assumptions of the pressure depth distributions result in an overestimation of the total force (the shadowed area), which became greater with increasing water depth. For 45° incident waves, Table 2 shows that for on-shore pressure force the over-estimations due to linear assumptions were about 10% at $d=20\text{m}$ to 19% at $d=40\text{m}$ greater than those due to theoretical profiles. They became even greater for the cases with normal incident waves, e.g. 46% and 26% for both 2nd and 3rd approximations. Overall, the over-estimations calculated by both approximations became closer in deep waters. This trend was also true for off-shore pressure force calculations. Therefore, linear assumptions always resulted in over-estimations and were more significant with increasing water depths. Besides, both approximations gave closer values at $d=40\text{m}$ than at $d=20\text{m}$, confirming the application of either of the two perturbed approximations in deeper water will not make much differences to each other.

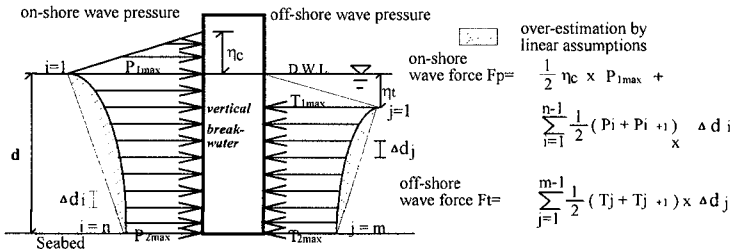


Figure 8. Definition Sketch for Design Short-Crested Wave Force Model

A Design Short-Crested Wave Force Model

According to above discussions, for a deep-water vertical breakwater we propose a design force model based on Fenton’s short-crested wave theory as schematically displayed in Figure 8. This model assumes that the residual surface pressure (on-shore) are negligible and set to be zero at the elevation of η_c . The pressures increase linearly to the maximum pressure at DWL (P_{1max}) such that the total wave pressure force above DWL is equal to the summation of each component pressure forces in the enclosed triangle area. The under water pressure force for both on and off-shore directions is the summation of the discrete unit pressure force derived directly from the theory for avoiding the over-estimations due to linear approximations. As a result, the total on and off-shore wave pressure forces at each depth calculated by this design wave force model were summarized in Table 2. Table 2 illustrated that by this design wave force model the results were slightly different from those by Eq. 6 at water depths.

Comparisons of total pressure forces with depth

The comparisons with Goda’s formulae will mainly focus on the on-shore total

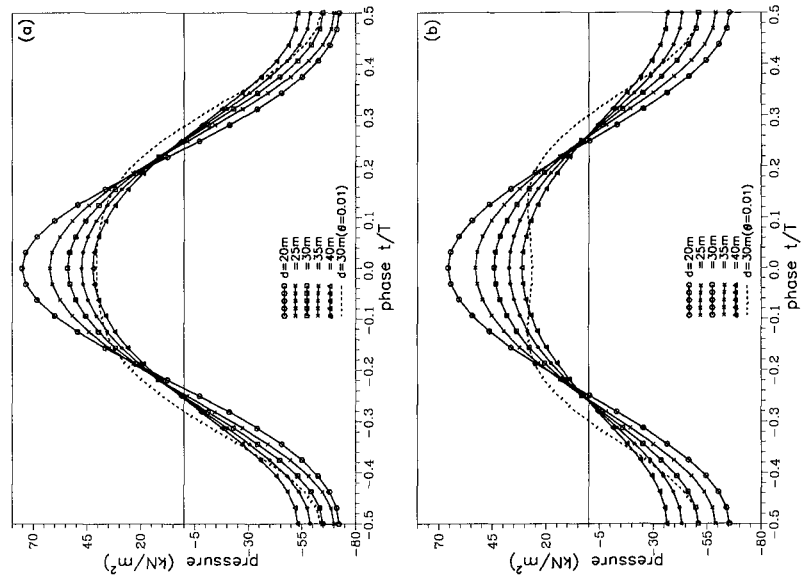


Figure 4. Pressure Variations with Phase at (a) Mid-Depth, (b) Seabed by 2nd-Order Approx. ($\theta=45^\circ$)

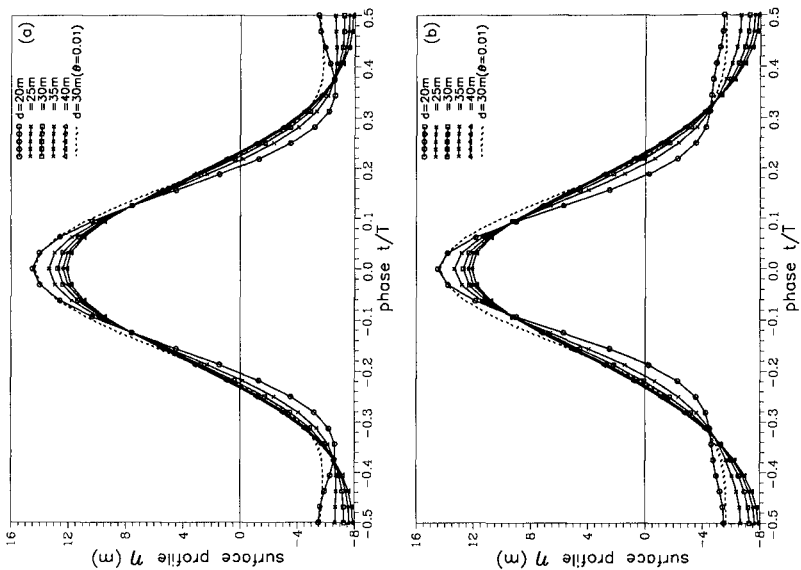


Figure 3. Surface Displacement with Phase by (a) 2nd-, (b) 3rd-Order S-C Wave Approx. ($\theta=45^\circ$)

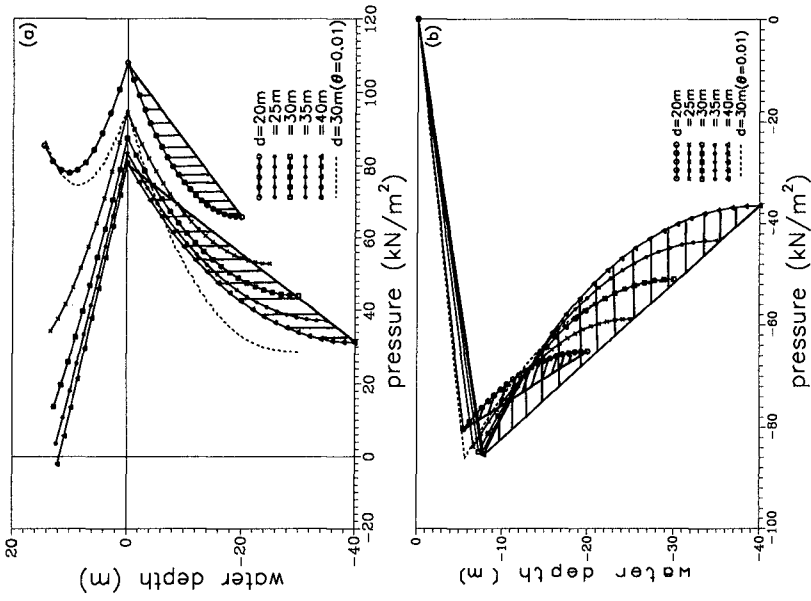


Figure 6. Vertical Distributions of S-C (a) On-, (b) Off-Shore Wave Pressures by 2nd-Order Approx. ($\theta=45^\circ$)

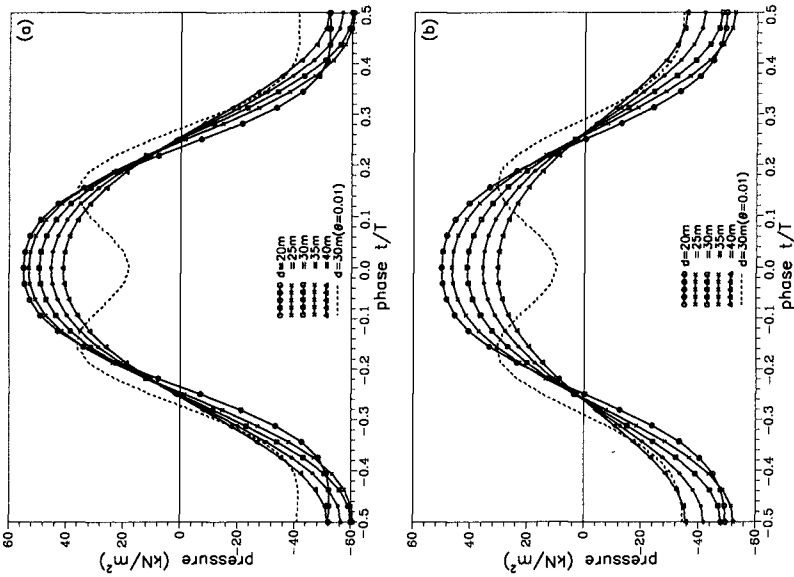


Figure 5. Pressure Variations with Phase at (a) Mid-Depth, (b) Seabed by 3rd-Order Approx. ($\theta=45^\circ$)

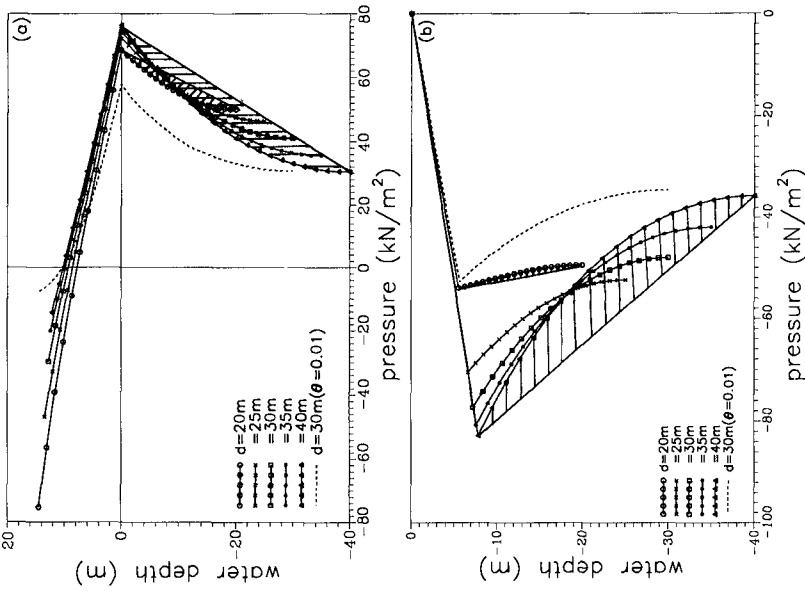


Figure 7. Vertical Distributions of S-C (a) On-, (b) Off-Shore Wave Pressures by 3rd-Order Approx. ($\theta=45^\circ$)

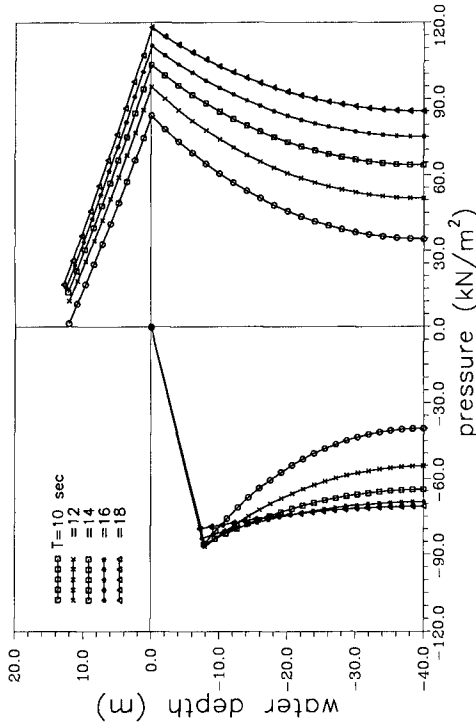


Figure 9. Vertical Distributions of S-C Wave Pressures with Period at $d=40\text{m}$ by 2nd-Order Approx. ($\theta=45^\circ$)

Table 2 Comparisons of Wave Forces on A Vertical Breakwater(unit : kN/m; $H_{\max}=10\text{m}$, $T=9.6\text{sec}$)

water depth (m)		20	25	30	35	40	30	40	
F above DWL		On-shore wave force ($\theta=45^\circ$)					($\theta=0^\circ$)		
(1) corrected	(3rd)	496.7	482.5	474.0	467.7	462.7	415.5	413.7	
	(2nd)	783.5	630.8	557.3	515.5	489.2	683.0	643.9	
(2) error ΔF	(3rd)	546.5	312.6	189.3	123.9	86.6	200.7	180.0	
	(2nd)	-466.7	-167.8	-56.2	-3.59	24.8	-472.2	-330	
Goda's		547.0	516.0	492.9	477.5	468.4			
F below DWL									
(3) curved	(3rd)	1129.5	1382.4	1567.9	1706.4	1808.9	1161.3	1274.2	
	(2nd)	1581.9	1652.3	1737.1	1813.2	1874.4	1429.8	1510.1	
(4) linear	(3rd)	1185.0	1483.6	1732.2	1946.1	2134.8	1327.5	1613.4	
	(2nd)	1737.1	1841.9	1973.1	2107.0	2236.8	1855.1	2211.2	
$\Delta F=(3)-(4)$		55.5	101.2	164.3	239.7	325.9	166.2	339.2	
$\Delta F / (3)$	(3rd)	(4.9%)	(7.3%)	(10.5%)	(14.0%)	(18.0%)	(14.3%)	(26.6%)	
	(2nd)	155.2	189.6	236	293.8	362.4	425.3	701.1	
		(9.8%)	(11.5%)	(13.4%)	(16.2%)	(19.3%)	(29.7%)	(46.4%)	
Goda's		1166.4	1305.9	1416.3	1528.9	1603.8			
Total wave force									
(5) (1) + (3)	(3rd)	1626.2	1864.9	2041.9	2174.0	2271.6	1576.8	1687.9	
	(2nd)	2365.4	2283.1	2294.4	2328.7	2363.6	2112.8	2145.0	
(6) Fenton's	(3rd)	1897.2	2023.9	2143.4	2242.3	2319.0	1427.7	1495.7	
	(2nd)	2086.5	2156.9	2241.6	2317.5	2378.6	1919.6	1927.3	
(7) Goda's		1713.4	1821.9	1909.3	2006.5	2072.2			
$\Delta F=(5)-(6)$		-271.0	-159.0	-101.5	-68.2	-47.3	-149.1	-192.2	
$\Delta F / (6)$	(3rd)	(-14.3%)	(-7.9%)	(-4.7%)	(-3.0%)	(-2.0%)	(-10.4%)	(-11.4%)	
	(2nd)	228.9	126.2	52.8	11.2	-15	193.2	217.7	
		(11.0%)	(5.9%)	(2.4%)	(0.5%)	(-0.6%)	(10.1%)	(11.3%)	
$\Delta F=(5)-(7)$		-87.3	43	132	167	199.5	-332.2	-416.4	
$\Delta F / (7)$	(3rd)	(-5.1%)	(2.4%)	(6.9%)	(8.3%)	(9.6%)	(-17.4%)	(-20.1%)	
	(2nd)	652	461.2	385.1	322.2	291.4	203.5	40.7	
		(38%)	(25.3%)	(20.2%)	(16.1%)	(14.1%)	(10.7%)	(2.0%)	
		Off-shore Wave Force($\theta=45^\circ$)					($\theta=0^\circ$)		
(8) curved	(3rd)	-743.2	-1073.3	-1308.0	-1483.4	-1614.7	-984.8	-1309.8	
	(2nd)	-1018.2	-1228.8	-1405.1	-1545.0	-1654.0	-1521.8	-1797.6	
(9) linear	(3rd)	-750.7	-1128.3	-1425.0	-1678.8	-1903.9	-1063.0	-1511.4	
	(2nd)	-1054.9	-1308.4	-1543.1	-1758.1	-1955.7	-1674.6	-2116.9	
$\Delta F=(8)-(9)$	(3rd)	46.8	55	117	195.4	289.2	78.2	201.6	
	(2nd)	36.7	79.6	138	213.1	301.7	152.8	319.3	

(2nd) and (3rd) denote results by Fenton's 2nd and 3rd-order approximations, respectively

Table 3 Summations of Short-Crested Swell Characteristics

$H_p=10m, d=40m, \theta=45^\circ$					
wave period T (sec)	10	12	14	16	18
wave crest elevation η_c (m)	12.095	12.071	12.22	12.50	12.87
wave trough elevation η_t (m)	-7.91	-7.93	-7.78	-7.51	-7.14
pressure at crest $P_{crest}(kN/m^2)$	-12.76	-7.28	-3.721	-0.86	1.80
	1.30	10.06	13.43	15.23	16.47
max. on-shore pressure at DWL	78.14	86.50	93.68	100.32	106.87
$P1_{max}$ (kN/m ²)	83.42	94.74	103.42	110.90	117.96
max. on-shore pressure at seabed	33.70	48.47	60.20	69.73	77.90
$P2_{max}$ (kN/m ²)	34.64	50.7	63.89	75.10	85.10
max. off-shore pressure at trough	-81.81	-81.66	-79.01	-75.16	-70.28
$T1_{max}$ (kN/m ²)	-85.86	-87.05	-86.14	-83.69	-80.00
max. off-shore pressure at seabed	-39.15	-52.91	-60.69	-63.94	-63.87
$T2_{max}$ (kN/m ²)	-40.08	-55.10	-64.38	-69.31	-71.08
$\Delta F_p = F_p(\text{linear}) - F_p(3rd)$	313.9	265.7	234.6	215.5	205
$\Delta F_p / F_p(3rd)$	(16.3%)	(10.9%)	(8.3%)	(6.8%)	(5.9%)
$\Delta F_p = F_p(\text{linear}) - F_p(2nd)$	345.4	321.9	285.6	256.7	233.7
$\Delta F_p / F_p(2nd)$	(17.3%)	(12.4%)	(9.3%)	(7.4%)	(6.1%)
Total on-shore wave force F_p	2395.5	2955.8	3415.4	3812.5	4178.1
	2500.3	3158.7	3692.5	4156.4	4586.6
$\Delta F_p = F_p(2nd) - F_p(3rd)$	104.8	202.9	277.1	343.9	408.5
$\Delta F_p / F_p(3rd)$	(4.4%)	(6.9%)	(8.1%)	(9.0%)	(9.8%)
Goda's design pressure force	2134.9	2524.8	2903.5	3250.3	3565.3
$\Delta F_p = F_p(3rd) - F_p(\text{Goda})$	260.6	431	511.9	562.2	612.8
$\Delta F_p / F_p(\text{Goda})$	(12.2%)	(17.1%)	(17.6%)	(17.3%)	(17.2%)
$\Delta F_p = F_p(2nd) - F_p(\text{Goda})$	365.4	633.9	789.0	906.1	1021.3
$\Delta F_p / F_p(\text{Goda})$	(17.1%)	(25.1%)	(27.2%)	(27.9%)	(28.6%)
Total off-shore wave force	-1694.6	-1997.1	-2152.2	-2201.1	-2171.5
(hydrodynamic components)	-1743.6	-2097.2	-2304.7	-2407.9	-2435.0
$\Delta F_T = F_T(\text{linear}) - F_T(3rd)$	-246.2	-160.7	-98.4	-58.6	-32.6
$\Delta F_T / F_T(3rd)$	(14.5%)	(8.0%)	(4.6%)	(2.7%)	(1.5%)
$\Delta F_T = F_T(\text{linear}) - F_T(2nd)$	-277.1	-182.2	-120.2	-77.6	-47.2
$\Delta F_T / F_T(2nd)$	(15.9%)	(8.7%)	(5.2%)	(3.2%)	(1.9%)

Note : the shadowed areas denote the calculations by the 3rd-order approximations

wave pressure forces in the following sections. The short-crested wave pressure forces were derived according to Figure 8 and standing wave pressure forces were based on Figure 1. From Table 2, the calculated total pressure forces by short-crested wave model were always greater than Goda's results, even though the over-estimation due to linear short-crested wave pressure distribution under DWL had been excluded. As water depths increased, the trends of depth distribution of wave pressure were opposite for both approximations and resulting total wave forces by 2nd-order were also greater than those by 3rd-order but the differences became smaller in deeper waters. At water depth of 40m, for example, the 45° incident short-crested waves could impose 10% to 14% greater pressure forces than standing waves on a vertical breakwater. Based on the findings and Table 2, it is expected that short-crested wave forces could still be significantly greater than standing waves forces at water depths over 40m. It is clearer that Goda's formulae tend to under-estimate total pressure forces especially for a deep-water vertical breakwater. Therefore, the traditional acknowledgment of standing waves to be the maximum imposing loading on a vertical breakwater should be corrected for future engineering practices.

Applications to short-crested swells

To further demonstrate the differences between current model and Goda's formulae, we shall briefly examine the variations of total wave pressure forces with longer waves at depth of 40m. The wave height is the same as discussed above but wave periods will be 10, 12, 14, 16, and 18 seconds, respectively. Results calculated by both short-crested wave approximations were summarized in Table 3. Figure 9 displays the phase variation of maximum on and off-shore pressure depth distributions by the 2nd-order approximations. It is observed from Table 3 that wave crest elevations η_c were only slightly increasing with wave periods and standing η_c are all higher than short-crested η_c but the differences decreased with longer wave periods. Figure 9 shows that the surface residual pressures were relatively small and Table 3 confirms the same trend for 3rd-order approximations. Besides, at this depth the curvature of the under-DWL on and off-shore pressure depth distributions were more significant for shorter-period waves by both approximations. Thus, the over-estimation by linear assumptions of the on-shore pressure depth distributions became less important such as were about 17.3% for T=10s to 6.1% for T=18s, respectively for 2nd-order approximations. But the variances in total wave forces derived according to Figure 8 between the two approximations became more significant with longer wave period. From Table 3, the total wave forces by 2nd-order were greater than those by 3rd-order approximations by about 4.4% for T=10s to 9.8% for T=18s. As a result for 45° incident short-crested waves acting on a vertical breakwater in such conditions, the total wave forces calculated by current model became greater with period than those by Goda's. For 3rd-order approximations, the trend could grow up about from 12% for T=10s to 17% for T=18s and became even more significant for those by 2nd-order approximations. The comparisons clearly suggest that the design forces could be under-estimated by Goda's formulae, especially in deep waters.

Conclusions and Suggestions

The evaluations with $\theta=45^\circ$ incident waves of $H_D=10\text{m}$ and $T=9.6\text{s}$ show that both Fenton's 2nd and 3rd-order approximations can be reasonably applicable at deep depths due to more negligible residual pressures at wave crest. Modified from the theory, present short-crested wave force model for deep-water vertical breakwaters defines maximum wave pressure P at DWL and linear distribution of P to zero pressure at wave crest. The resulting wave pressure forces are simply the summations of pressure distributions derived according to theoretical approximations at discrete depths. Linear assumptions for pressure depth distribution under DWL result in greater over-estimated total wave forces with increasing water depth or shorter waves. Differences between 2nd and 3rd-order approximations always become negligible as water depth increased but more significant for longer waves or for $\theta=0^\circ$. For $\theta=45^\circ$ and $T=9.6\text{s}$, the over-estimations by 3rd-order approximations could amount about from 5% to 18% at $d=20\text{m}$ to 40m but then decrease to 6% for $T=18\text{s}$ at $d=40\text{m}$. For current wave conditions, Goda's formulae for standing waves under-estimate the total pressure forces than short-crested waves of $\theta=45^\circ$ by at least 10% at depth of 40m and up to 17% or 28% for waves of $T=18\text{s}$ derived by 3rd-order and 2nd-order approximations, respectively.

It is recommended that more studies on the applications of the current model to field conditions to be carried out for further design needs of deep-water breakwaters. Three-dimensional hydraulic model tests are considered necessary for decisive selection between the two approximations. Further extension to establish a similar model for composite breakwaters will be very valuable for engineering practices.

References

- Chappellear, J. E. (1961), "On the description of short-crested waves," *Beach Erosion Bd, U.S. Army Corps Engrs. Tech. Memo*, No. 125.
- Fenton, J. D.(1985), "Wave forces on vertical walls," *J. of Waterway, Port, Coastal and Ocean Engineering*, Vol. 111, No. 4, pp. 193-717.
- Goda, Y. (1972), "New wave pressure formulae for composite breakwater," *Proc. of 14th Int. Conf. Coastal Engineering*, Copenhagen, pp. 1702-1720.
- Goda, Y. (1985), *Random Sea Waves and Engineering Applications*, University of Tokyo Press, Ch4.
- Hsu, J. R. C., Y. Tsuchiya, and R. Silvester (1979) "Third-order approximation to short-crested waves," *J. Fluid Mech.*, Vol. 90, No. 1, pp. 179-196.
- Jeffreys, H. (1924), "On water waves near the coast," *Phil. Mag. Ser.*, Vol. 6, No. 48, pp. 44-48.
- Roberts, A. J. and L. W. Schwartz, (1983) "The calculation of non-linear short-crested gravity waves," *Phys. Fluids*, Vol. 26, No. 9, pp. 2388-2392.
- Silvester, R.(1974), *Coastal Engineering*, Vol. 1, Elsevier, Amsterdam, Netherlands.
- Tanimoto, K. and S. Takahashi, (1994), "Design and construction of caisson breakwaters - the Japanese experience," *Coastal Engineering*, Vol. 22, pp. 55-77.